Environmental Science and Pollution Research
https://doi.org/10.1007/s11356-023-30572-y

RESEARCH ARTICLE

County-level artificial light at night (ALAN) in the contiguous US (2012–2019): spatial variations, temporal trends, and environmental justice analyses

Qian Xiao[1,4] · Meng Zhou[2] · Yue Lyu[3] · Jiachen Lu[3,4] · Kehe Zhang[3,4] · Mariana Figueiro[5] · Jun Wang[2] · Cici Bauer[3,4]

Received: 8 May 2023 / Accepted: 16 October 2023

Abstract
Artificial light at night (ALAN) is a growing environmental hazard with economic, ecological, and public health implications. Previous studies suggested a higher burden of light pollution and related adverse effects in disadvantaged communities. It is critical to characterize the geographic distribution and temporal trend of ALAN and identify associated demographic and socioeconomic factors at the population level to lay the foundation for environmental and public health monitoring and policy-making. We used satellite data from the Black Marble suite to characterize ALAN in all counties in contiguous US and reported considerable variations in ALAN spatiotemporal patterns between 2012 and 2019. As expected, ALAN levels were generally higher in metropolitan and coastal areas; however, several rural counties in Texas experienced remarkable increase in ALAN since 2012, while population-level ALAN burden also increased substantially in many metropolitan areas. Importantly, we found that during this period, although the overall ALAN levels in the USA declined modestly, the temporal trend of ALAN varied across areas with different racial/ethnic compositions: counties with a higher percentage of racial/ethnic minority groups, particularly Hispanic populations, exhibited significantly less decline. As a result, the differences in ALAN levels, as measured by the Black Marble product, across racial/ethnic groups became larger between 2012 and 2019. In conclusion, our study documented variations in ALAN spatiotemporal patterns across America and identified multiple population correlates of ALAN patterns that warrant further investigations. Future studies should identify underlying factors (e.g., economic development and decline, urban planning, and transition to newer lighting technologies such as light emitting diodes) that may have contributed to ALAN disparities in the USA.

Keywords Artificial light at night · Geographic variation · Temporal trend · Environmental justice

Responsible Editor: Philippe Garrigues

✉ Qian Xiao
qian.xiao@uth.tmc.edu

1 Department of Epidemiology, Human Genetics and Environmental Sciences, School of Public Health, The University of Texas Health Science Center at Houston, Houston, TX 77030, USA

2 Department of Chemical and Biochemical Engineering, University of Iowa, Iowa City, IA, USA

3 Department of Biostatistics and Data Science, The University of Texas Health Science Center at Houston, Houston, TX, USA

4 Center for Spatial-Temporal Modeling for Applications in Population Sciences, Houston, TX, USA

5 Light and Health Research Center, Department of Population Health Science and Policy, Icahn School of Medicine at Mount Sinai, New York, NY, USA

Introduction

Over the past century, global nightscapes have been drastically changed by the rapid growth of electric lighting. It is estimated that ALAN has grown by up to 20% annually in many urban areas since the mid-twentieth century (Hölker, Moss et al. 2010). A more recent analysis using data gathered by the Visible Infrared Imaging Radiometer Suite Day-Night Band (VIIRS DNB) reported that not only have the total lit areas (defined as radiance>5 $nWcm^{-2}\ sr^{-1}$) expanded considerably around the globe between 2012 and 2016, brightness levels in areas that were already continuously lit increased by 2.2% per year during this period (Kyba, Kuester et al. 2017). According to one estimate, more than 99% of the US population now live in areas with light-polluted skies (Falchi, Cinzano et al. 2016).

Although electric lighting has tremendous benefits, including promoting commercial activities, social interactions, and public safety, these benefits are also accompanied by negative economic, ecological, and public health consequences. Higher levels of ALAN cause higher energy cost, greater greenhouse gas emissions, and detrimental effects to the natural environment and ecosystems (Falchi, Cinzano et al. 2011, Cao and Bai 2014, Gaston, Visser et al. 2015, Ou, Liu et al. 2015, Li, Elvidge et al. 2017, Román, Wang et al. 2018, Song, Wang et al. 2021). Moreover, as pointed out by an expert panel convened by the National Toxicology Program, ALAN can both directly affect human circadian regulation and enable nighttime activities that disrupt natural sleep-wake and eating-fasting cycles (Lunn, Blask et al. 2017). Indeed, growing evidence from basic and clinical studies have linked excessive ALAN with a wide range of adverse health outcomes, including obesity, diabetes, cardiovascular disease, cancer, and cognitive and mental disorders (Lunn, Blask et al. 2017, Mason, Boubekri et al. 2018). Given that ALAN is one of the most ubiquitous environmental exposures with a wide societal impact, it is critical to monitor its geographic distribution and temporal trend to provide fundamental knowledge and lay the foundation for lighting-related policy-making.

Several recent studies investigated global patterns of ALAN, and some specifically focused on the USA (Falchi, Cinzano et al. 2016, Kyba, Kuester et al. 2017, Falchi, Furgoni et al. 2019, Elvidge, Hsu et al. 2020). However, only one of these studies reported the ALAN levels at the administrative units (e.g., county) (Falchi, Furgoni et al. 2019), where key socioeconomic and public health statistics are typically reported and where policy change often occurs, and this study did not focus on temporal trends. Moreover, at least one earlier study reported higher levels of exposure among racial/ethnical minority groups and low socioeconomic (SES) populations, suggesting that ALAN is an environmental justice (EJ) issue (Nadybal, Collins et al. 2020). However, to the best of our knowledge, no study has examined whether and how *temporal trends* of ALAN vary across different demographic and socioeconomic groups. Taken together, there is a need for studies that characterize both the temporal trend and geographic distribution of ALAN, and that examine the correlating population-level attributes in the USA. Findings from such investigations will help identify communities with high ALAN exposures and rapid increases in ALAN, motivate further investigation of the underlying causes of unequal ALAN patterns, guide monitoring efforts, and provide evidence to support policy change.

The primary objectives of this study are (1) to derive yearly ALAN measures for all US contiguous counties between 2012 and 2019, (2) to identify counties with the highest and lowest average ALAN exposures and with the largest increases and decreases in ALAN during this period, and (3) to study the associations of multiple demographic and socioeconomic factors (i.e., population, gross domestic product (GDP), racial/ethnic composition, and poverty rate) with ALAN spatiotemporal patterns.

Methods

Satellite-based ALAN quantification

Yearly, ALAN in the contiguous US between 2012 and 2019 was measured using NASA's fourth nighttime lights product in the Black Marble suite (VNP46A4) (Román, Wang et al. 2018, Wang, Shrestha et al. 2022), which provides annual composite measures of ALAN based on daily nighttime visible measurements from the VIIRS DNB sensor aboard the Suomi NPP satellite. VIIRS DNB is a panchromatic sensor that is ultrasensitive in low-lit conditions and can detect light in the visible and near-infrared spectrum at a resolution of ~750 m. Nighttime was defined as the solar zenith angle of 108° or larger. The black marble algorithm was applied to the VIIRS DNB observation to produce cloud-free and atmospheric-, terrain-, vegetation-, snow-, lunar-, and stray light-corrected radiance data in 15 arc-second linear latitude and longitude grid (~500 m in mid-latitude). Because recent studies have shown that ALAN measure is affected by the blockage and vertical visibility effects of buildings (Tan, Zhu et al. 2022), we used the annual composite dataset (VNP46A4) consisting of averaged observations from all angles upon snow-free land surface throughout the year. The VNP46 product enables the detection of ALAN change at different temporal levels, from daily to annual changes (Román, Wang et al. 2018).

The shapefile containing annual ALAN information was mapped onto all counties in the contiguous US. All data processing and mapping were performed using R (Voelkel, Hellman et al. 2018). County-level ALAN data are now published and publicly available (https://disc.gsfc.nasa.gov/datasets/ALAN_VIIRS_CONUS_1/summary).

Characterizing county-level ALAN spatiotemporal patterns

We derived two measures of ALAN for each county and year: county-level average ALAN and population-level ALAN burden. The former was derived as the average of ALAN of all grids within a county's geographical boundary, while the latter was calculated as the former multiplied by the total population size of the county given a specific year, i.e., ALAN × population (1000). We then calculated average values for both indicators for the period of 2012–2019.

We used a mixed-effect multivariable linear regression model to provide model-based estimates of the temporal changes in ALAN by county between 2012 and 2019. County-level ALAN was highly skewed to the right, so we performed the log transformation to improve normality for both outcome variables. Specifically, let $y_{i[s]t}$ denote the ALAN radiance (on log scale) for county i in state s (hence, the notation $i[s]$) for year t. We modeled the time series of $y_{i[s]t}$ with:

$$y_{i[s]t} = \alpha + \beta_s \text{State}_s + \beta_t \text{Year}_t + \left(\beta_{0i} + \beta_{1i}\text{Year}_t\right) + \epsilon_{i[s]t},$$

where α was the intercept, β_s the fixed effect of the mean ALAN radiance for a specific State (State_s), and β_t the fixed effect of the mean ALAN radiance for a specific year (Year_t). To capture the county level variation of the average ALAN level and temporal change, we included the random intercept β_{0i} and temporal slope β_{1i} assuming normal distributions with respective variances. The residuals $\epsilon_{i[s]t}$ were assumed to have independently and identically distributed normal distributions. The county-specific coefficient for year was exponentiated to measure % annual changes in ALAN. To determine the population exposure to ALAN change within a county, we multiplied the annual rate of ALAN change with the average population (1000) within a county between 2012 and 2019.

Determining the relationship between demographic and socioeconomic factors and ALAN

To study population-level demographic and socioeconomic factors in relation to ALAN, we focused on two variables with a well-established relationship with ALAN (GDP and population size) and several variables that have not been extensively studied in relation to ALAN (% of racial/ethnic minority population, % of Black population, % of Hispanic population, and % of population living under the federal poverty level). For the former group, we presented county-level GDP and population size with average ALAN and changes in ALAN for descriptive purposes. We also calculated the correlation coefficients between GDP and population size and ALAN, as well as the % variance in ALAN explained by these two factors. For the latter group, the objective was to determine average levels and temporal trajectories of ALAN across counties with different racial/ethnic compositions and poverty rates. We used the aforementioned linear mixed model that additionally included the county-year specific demographic or socioeconomic variable (e.g., poverty rate) and an interaction term between this variable and the year. We presented coefficients for both the main effect and the interaction term, and we plotted the predicted least squares means of ALAN (back transformed from log(ALAN) to geometric means) to demonstrate different ALAN trajectories for each quintile of the demographic or socioeconomic variable of interest.

Results

Figure 1A presents a composite nighttime image of the USA and neighboring countries in 2019. Average ALAN levels between 2012 and 2019 in all counties in the contiguous US are presented in Figure 1B. We observed substantial spatial variation in ALAN levels among US counties. Overall, ALAN levels were higher in the east regions than the west and particularly high in counties along the coasts. As expected, ALAN levels were higher in large metropolitan areas while lower in rural counties.

Table 1 lists the top ten counties with the *highest* average ALAN levels and population-level ALAN burden (defined as ALAN × population (1000)) separately (Supplementary Table 1 presents average ALAN and population-level ALAN burden for all counties). When ranked by average ALAN levels, the top 10 counties were primarily located in large metropolitan areas on the east coast, with Washington DC ranking the highest. When ranked by the population-level ALAN burden, the highest was Cook County in Illinois (including the City of Chicago), followed by Harris County in Texas (including the City of Houston). Counties with the *lowest* average levels of ALAN and population-level ALAN burden are presented in Table 2. Catron County in New Mexico had the lowest level of the average ALAN, while Petroleum County in Montana had the lowest ALAN burden. All counties listed in Table 2 were rural counties located in midwestern, southwestern, and western states, including New Mexico, Montana, Colorado, Nebraska, Michigan, Texas, and Oregon.

Between 2012 and 2019, the ALAN in the contiguous US decreased by ~3% per year (β (95% CI), −0.029 (−0.030, −0.027)). Temporal changes in ALAN in all US states are presented in Supplementary Figure 1, with most states showing a stable trend or slight decreases. Temporal changes in ALAN at the county level are presented in Figure 2. Most counties across the country showed a modest decrease in ALAN. However, some counties, particularly several in the western Texas, showed a large increase.

Table 3 presents the top ten counties with the largest annual increases in ALAN and population exposure to ALAN (defined as annual change in ALAN × population (1000)), separately (Supplementary Table 1 presents annual change in ALAN and population exposure to ALAN change for all counties). Strikingly, when ranked by annual increase in ALAN relative to all other counties, all top 10 counties were in Texas. The highest increase was observed in Loving County, Texas, with an average rate at 50.46% per year, and the rest all had an annual rate of increase higher than

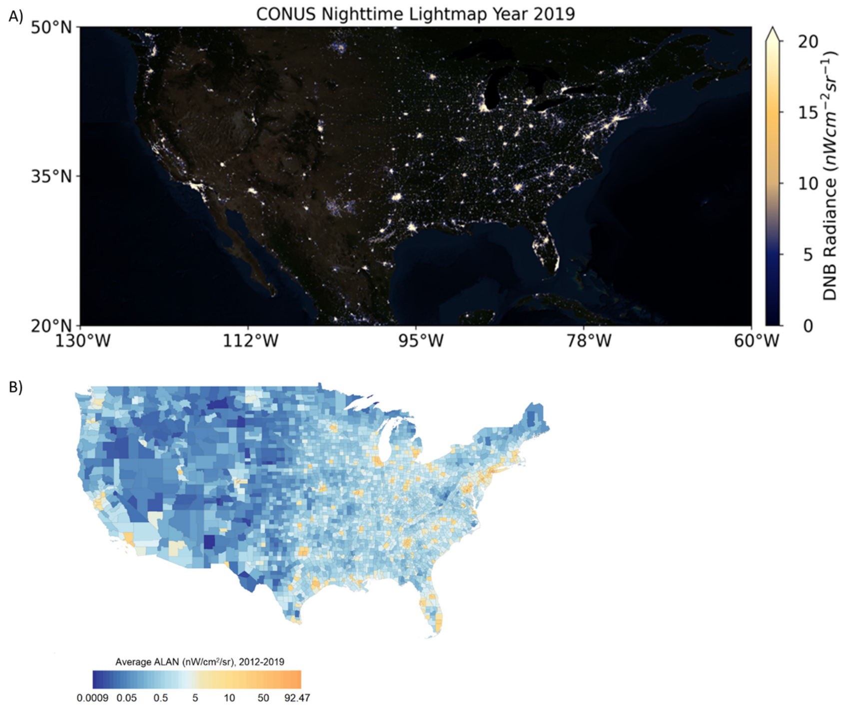

Fig. 1 Artificial light at night levels (ALAN) in the USA. **A** Satellite image of the contiguous US at night in 2019, using NASA's Black Marble Product based on data gathered by the Visible Infrared Imaging Radiometer Suite Day-Night Band. **B** Eight-year (2012–2019) average of mean ALAN in US counties. Abbreviations: CONUS, contiguous US; DNB, Day-Night Band

Table 1 US counties with the highest ALAN exposure (2012–2019)

State	County	Average ALAN ($nW/cm^2/sr$)	Average population-level ALAN burden[a]	Average population (1000)	Average GDP (1000$ in 2012 dollars)
Top 10 counties based on ALAN, 2012–2019 average					
District of Columbia	District of Columbia	92.47	60,197.45	651.87	117,933,678
New York	New York	80.44	130,773.98	1625.41	586,685,001
Missouri	St. Louis	70.31	22,198.74	315.55	27,253,558
Maryland	Baltimore	66.64	41,249.49	618.92	43,988,986
New Jersey	Hudson	61.58	40,708.69	660.66	42,125,135
Pennsylvania	Philadelphia	58.89	91,619.70	1556.09	103,482,052
Virginia	Alexandria	57.43	8610.92	150.01	13,933,571
New York	Bronx	52.52	74,769.07	1423.90	40,441,612
New York	Kings	48.23	124,464.67	2581.41	84,221,163
New York	Queens	45.39	103,843.00	2288.54	87,934,066
Top 10 counties based on population-level ALAN burden[a], 2012–2019 average					
Illinois	Cook	30.38	158,605.64	5220.30	351,200,412
Texas	Harris	35.17	154,458.04	4389.87	361,278,873
California	Los Angeles	14.29	143,109.09	10,011.07	661,763,125
New York	New York	80.44	130,773.98	1625.41	586,685,001
New York	Kings	48.23	124,464.67	2581.41	84,221,163
New York	Queens	45.39	103,843.00	2288.54	87,934,066
Pennsylvania	Philadelphia	58.89	91,619.70	1556.09	103,482,052
Texas	Dallas	34.84	87,028.47	2498.04	220,169,207
New York	Bronx	52.52	74,769.07	1423.90	40,441,612
California	Orange	22.74	70,795.87	3112.03	213,231,652

[a]Defined as ALAN × population (1000) in each county

Abbreviations: *ALAN* artificial light at night, *GDP* gross domestic product

Table 2 US counties with the lowest ALAN exposure (2012–2019)

State	County	Average ALAN (nW/cm^2/sr)	Average population-level ALAN burden[a]	Average population	Average GDP (1000$ in 2012 dollars)
Bottom 10 counties based on ALAN, 2012–2019 average					
New Mexico	Catron	0.00090	3.25	3595.25	81,735
Montana	Petroleum	0.00124	0.61	477.38	29,996
Montana	Garfield	0.00144	1.57	1089.13	52,204
Colorado	Hinsdale	0.00155	1.30	844.38	36,912
Montana	Carter	0.00156	2.00	1276.63	81,872
Nebraska	McPherson	0.00164	0.67	411.88	33,337
Michigan	Keweenaw	0.00168	3.64	2164.50	44,038
New Mexico	Harding	0.00192	1.10	566.25	124,564
Texas	Jeff Davis	0.00199	4.50	2259.50	74,301
Oregon	Wheeler	0.00216	2.94	1363.63	32,527
Bottom 10 counties based on population-level ALAN burden[a], 2012–2019 average					
Montana	Petroleum	0.00124	0.61	477.38	29,996
Nebraska	McPherson	0.00164	0.67	411.88	33,337
New Mexico	Harding	0.00192	1.10	566.25	124,564
Colorado	Hinsdale	0.00155	1.30	844.38	36,912
Montana	Garfield	0.00144	1.57	1089.13	52,204
Nebraska	Arthur	0.00370	1.68	453.00	22,016
Montana	Carter	0.00156	2.00	1276.63	81,872
Texas	King	0.00950	2.57	266.63	194,572
Nebraska	Blaine	0.00485	2.65	544.25	44,892
Colorado	Mineral	0.00350	2.66	771.75	55,881

[a]Defined as ALAN × population in each county

Abbreviations: *ALAN* artificial light at night, *GDP* gross domestic product

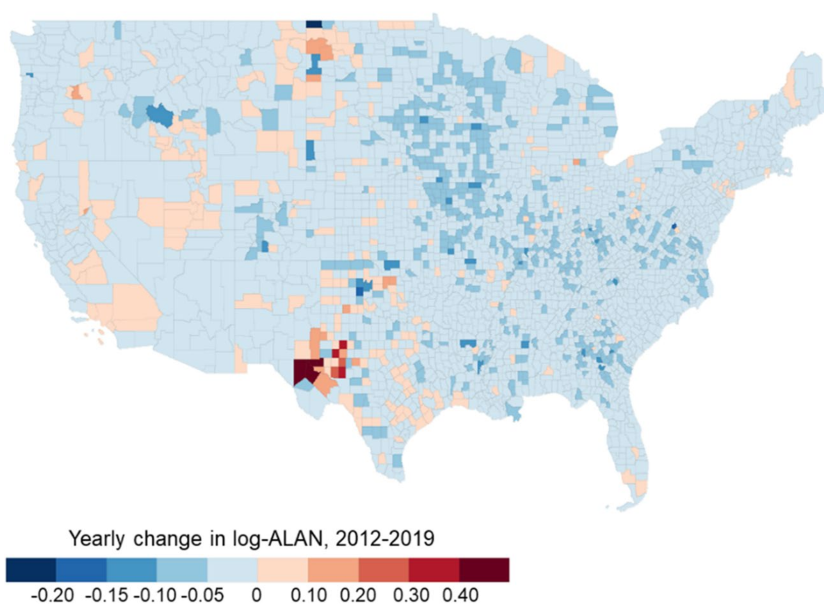

Fig. 2 Yearly changes in ALAN between 2012 and 2019 in all counties in the contiguous US

Table 3 US counties with the largest increase in ALAN exposure (2012–2019)

State	County	Annual change in ALAN, %	Population exposure to ALAN change [a]	Total change in population, %	Total change in GDP, %	Average population (1000)
Top 10 counties based on annual increase in ALAN, 2012–2019						
Texas	Loving	50.46%	0.05	15.29%	1252.59%	0.091
Texas	Winkler	45.14%	3.42	10.23%	187.67%	7.57
Texas	Culberson	45.01%	1.03	−7.21%	803.48%	2.29
Texas	Reeves	43.61%	6.29	13.86%	1079.15%	14.42
Texas	Martin	39.04%	2.07	17.59%	325.95%	5.30
Texas	Reagan	35.46%	1.28	11.29%	279.51%	3.60
Texas	Borden	35.22%	0.23	−4.52%	73.86%	0.66
Texas	Upton	32.61%	1.13	10.88%	147.13%	3.46
Texas	Glasscock	32.35%	0.42	20.32%	171.72%	1.30
Texas	Ward	22.56%	2.54	8.90%	89.71%	11.24
Top 10 counties based on population exposure to ALAN increase[a], 2012–2019						
California	Los Angeles	3.39%	339.40	2.45%	22.70%	10011.07
Texas	Harris	3.58%	157.00	13.28%	14.44%	4389.87
California	Orange	4.17%	129.66	4.84%	20.51%	3112.03
Arizona	Maricopa	2.59%	105.21	12.68%	23.63%	4065.41
Florida	Miami-Dade	3.87%	101.91	7.45%	28.18%	2635.40
California	Riverside	4.40%	101.53	9.96%	30.12%	2307.51
California	San Diego	3.09%	99.78	6.95%	23.27%	3225.12
Texas	Dallas	3.30%	82.42	9.57%	24.37%	2498.04
California	San Bernardino	3.87%	81.10	5.29%	29.05%	2097.96
Texas	Tarrant	3.83%	74.09	12.96%	15.88%	1932.50

[a]Measured as annual change in ALAN (%) × average population (1000)

Abbreviations: *ALAN* artificial light at night, *GDP* gross domestic product

20%. When ranked by increase in population exposure to ALAN, all top 10 counties were from large metropolitan areas, led by Los Angeles County, followed by four other counties in California (Orange, Riverside, San Diego, San Bernardino), three in Texas (Harris, Dallas, Tarrant), one in Arizona (Maricopa), and one in Florida (Miami-Dade). Table 4 lists the top counties with the largest decreases in ALAN and population exposure to ALAN. When ranked by changes in ALAN, Divide County, North Dakota, had the largest decrease of 16.83%. Most of these counties were rural counties from midwestern and southern states. When ranked by population exposure to ALAN change, Pima County in Arizona showed the largest decrease, primarily driven by its large population size. Other counties ranked among the top 10 list were small metropolitan and nonmetropolitan urban areas.

We studied the association between ALAN and population size, GDP, racial/ethnic composition and poverty rate at the county level. Overall, there was high correlation between average ALAN and population size and GDP (Spearman's rank correlation coefficient $\rho = 0.80$ and 0.78, respectively). Moreover, there was moderate correlation between changes in ALAN and changes in population size (Pearson correlation coefficient $r = 0.37$) and changes in GDP ($r = 0.40$). Together, population and GDP explained 23.1% of the total variance in annual changes in ALAN across all counties. We found that racial/ethnic compositions and poverty rate were also associated with average and changes in ALAN (Table 5 and Figure 3). Specifically, ALAN trajectories varied significantly across counties with different racial/ethnic compositions: counties with the lowest concentration of racial/ethnic minority groups had the largest decline in ALAN over the study period, while counties with the highest concentration had the smallest decline (Figure 3A). Notably, in 2012, counties with a higher concentration of minority groups had lower levels of ALAN; however, this pattern reversed after 2014, and the gap in ALAN levels across quintiles of racial/ethnic composition continued to grow. As a result, in 2019, counties in the highest quintile of minority concentration had the highest ALAN levels. Analyses by % of Black (Figure 3B) and Hispanic (Figure 3C) populations showed that this pattern of reversed and widening gaps of ALAN across racial/ethnic concentrations was primarily driven by differences in ALAN trajectories across counties with

Table 4 US counties with the largest decrease in ALAN exposure (2012–2019)

State	County	Annual change in ALAN, %	Population exposure to ALAN change [a]	Total change in population, %	Total change in GDP, %	Average population (1000)
Top 10 counties based on annual decrease in ALAN, 2012–2019						
North Dakota	Divide	−16.83%	−0.38	11.46%	−28.82%	2.28
Texas	Wheeler	−13.53%	−0.75	−1.40%	−50.23%	5.53
Virginia	Rappahannock	−12.42%	−0.92	−0.83%	28.04%	7.41
North Dakota	Billings	−11.27%	−0.10	10.02%	50.09%	0.92
Iowa	Davis	−11.06%	−0.97	2.32%	13.88%	8.80
Iowa	Van Buren	−10.41%	−0.77	−5.49%	−12.31%	7.38
Louisiana	Catahoula Paris	−9.95%	−1.01	−6.18%	−19.27%	10.14
Oklahoma	Roger Mills	−9.78%	−0.36	−0.30%	−19.80%	3.72
Louisiana	Union Parish	−9.66%	−2.18	−1.24%	10.66%	22.52
Illinois	Pope	−9.54%	−0.41	−4.46%	−49.98%	4.32
Top 10 counties based on population exposure to ALAN decrease[a], 2012–2019						
Arizona	Pima	−0.53%	−5.33	4.71%	15.29%	1002.14
Wisconsin	Polk	−6.48%	−2.82	−1.49%	14.55%	43.61
Louisiana	Union Parish	−9.66%	−2.18	−1.24%	10.66%	22.52
Pennsylvania	Crawford	−2.42%	−2.11	−3.19%	3.45%	87.19
Pennsylvania	Bradford	−3.21%	−1.99	−2.66%	38.99%	61.95
Wisconsin	Dunn	−3.91%	−1.73	2.22%	2.68%	44.22
Minnesota	Fillmore	−7.60%	−1.59	0.33%	4.11%	20.87
Minnesota	Mower	−4.10%	−1.61	1.77%	−0.09%	39.37
New York	Allegany	−3.37%	−1.61	−4.40%	6.18%	47.84
Michigan	Sanilac	−3.72%	−1.56	−4.18%	14.20%	42.00

[a]Measured as annual change in ALAN (%) × average population (1000)

Abbreviations: *ALAN* artificial light at night, *GDP* gross domestic product

different Hispanic populations. In contrast, the association between % Black population and ALAN trajectories was less pronounced. Finally, although there was a statistically significant association between % poverty rate and ALAN, the effect sizes were small, and ALAN trajectories appeared to be largely similar across counties with different poverty levels (Figure 3D).

Discussion

We created yearly ALAN measures for all counties in contiguous US between 2012 and 2019 and reported substantial variation in both the geographical distribution of and temporal trend in ALAN during this period. As expected, average levels of ALAN were higher in large metropolitan areas and coastal regions and were strongly correlated with GDP and population size. During this period, although the ALAN at the national level decreased slightly since 2012, there existed considerable differences in ALAN trend over time across the country. Several rural counties in Texas experienced a remarkable increase in ALAN, while substantial increases in population exposure to ALAN were also observed in many metropolitan areas. Overall, changes in GDP and population size were important predictors of ALAN change, but the majority of variability in county-level ALAN trends was not explained by these two variables. Finally, we found that counties with the highest concentration of minority groups, especially Hispanics, experienced the least decrease in ALAN levels. As a result, racial/ethnic disparities in ALAN have grown wider since 2014 across the USA.

A number of earlier studies examined geographical distributions of ALAN levels globally and in the USA (Falchi, Cinzano et al. 2016, Kyba, Kuester et al. 2017, Falchi, Furgoni et al. 2019, Elvidge, Hsu et al. 2020). Like ours, most of these used data from the VIIRS DNB, which provides calibrated, high-resolution nighttime images with large dynamic range. At least one study (Falchi et al. 2019) examined county-level ALAN in the USA using 2014 VIIRS observations. Although the study used a somewhat different measure of ALAN (light flux from emitting sources), it produced county rankings of ALAN levels almost identical to ours. The study also revealed a dramatic difference (200,000-fold) between counties with the highest and lowest levels

Table 5 Associations of county-level racial/ethnic composition and poverty rate with average levels and temporal changes of ALAN in contiguous US (2012–2019)

	log (ALAN)		
		beta (95% CI)	
	Mean (SD)	Main effect	Interaction w/ year
% Racial/ethnic minority			
Q1	−1.49 (1.38)	Ref	Ref
Q2	−1.09 (1.52)	−0.05 (−0.066, −0.035)	0.013 (0.010, 0.016)
Q3	−0.62 (1.64)	−0.049 (−0.071, −0.027)	0.018 (0.015, 0.022)
Q4	−0.26 (1.69)	−0.029 (−0.057, −0.001)	0.019 (0.015, 0.023)
Q5	−0.21 (1.94)	−0.045 (−0.079, −0.011)	0.026 (0.022, 0.030)
% NH Black			
Q1	−2.34 (1.50)	Ref	Ref
Q2	−1.35 (1.32)	−0.015 (−0.025, −0.005)	0.004 (0.002, 0.007)
Q3	−0.55 (1.31)	−0.024 (−0.038, −0.01)	0.008 (0.005, 0.011)
Q4	0.30 (1.38)	−0.011 (−0.031, 0.008)	0.010 (0.007, 0.014)
Q5	0.22 (1.46)	0.041 (0.011, 0.072)	−0.001 (−0.005, 0.003)
% Hispanic			
Q1	−1.28 (1.41)	Ref	Ref
Q2	−0.87 (1.37)	−0.028 (−0.040, −0.015)	0.007 (0.005, 0.010)
Q3	−0.60 (1.64)	−0.057 (−0.073, −0.041)	0.014 (0.011, 0.017)
Q4	−0.30 (1.79)	−0.083 (−0.104, −0.063)	0.023 (0.019, 0.026)
Q5	−0.65 (2.10)	−0.072 (−0.100, −0.043)	0.033 (0.030, 0.037)
% Under poverty			
Q1	−0.93 (1.97)	Ref	Ref
Q2	−0.82 (1.73)	0.005 (−0.005, 0.015)	−0.002 (−0.004, 0.001)
Q3	−0.69 (1.72)	0.014 (0.002, 0.026)	−0.004 (−0.007, −0.001)
Q4	−0.51 (1.52)	0.021 (0.007, 0.034)	−0.006 (−0.008, −0.003)
Q5	−0.74 (1.44)	0.032 (0.017, 0.048)	−0.009 (−0.012, −0.005)

of ALAN, an estimate similar to that observed in our study (102,744-fold difference in average ALAN levels comparing Washington DC to Catron, New Mexico). Besides average ALAN, we also estimated population-level ALAN burden, a metric often used to assess public health impact of environmental contaminants such as air pollution (Moschandreas 2011), and reported a ~260,000-fold difference comparing counties with the highest and lowest population exposure (Cook, Illinois and Petroleum, Montana, respectively). Such vast differences in ALAN exposures suggest that the population-level health risks associated with ALAN are likely to vary widely across the country.

Although our study, to the best of our knowledge, is the first to provide comprehensive data on ALAN temporal changes at the county level in the USA, several previous studies estimated changes in ALAN in different world regions. For example, one paper summarized older studies using data from various sources to estimate ALAN change in the second half of the twentieth century and showed an annual increase rate between 2.5 and 19% in several urban areas in the USA, Europe, Asia, and Central America (Hölker, Moss et al. 2010). A more recent analysis by Kyba et al. estimated that the global expansion of artificially lit outdoor area was at an annual rate of 2.2% between 2012 and 2016, and for continuously lit areas (defined as average ALAN (2012–2016) ≥ 5 nW/cm^2/sr), the level of brightness on average also increased by 2.2% per year (Kyba, Kuester et al. 2017). Interestingly, this paper found that the USA had a stable trajectory in ALAN during this period, along with a few other high-income countries in Europe. We also found a largely stable and slightly downward trend in national ALAN level; however, this average trend does not reveal the substantial differences in ALAN temporal changes across different counties. Moreover, it is worth noting that patterns in changes in ALAN and in population-level ALAN burden were drastically different, with the latter largely influenced by population size. This difference is important to consider because different metrics of change may have different clinical and public health implications. For example, in rural areas such as Loving, Texas, the tremendous increase in ALAN levels may have a large impact on each individual in spite of the small population size. On the other hand, in more populated areas such as Los Angeles, California, even a small increase in ALAN levels may have a sizable public health impact due to its sheer population size. Finally, it is worth noting that the observed decline in certain areas may not reflect a true decline in ALAN levels. In the recent decade, the use of light emitting diodes (LED) technology has increased in many areas across the USA. Many LEDs emit light with a peak emission in the 400–500 nm range. However, the VIIRS DNB system lacks light sensitivity to wavelengths outside 500–900 nm and thus may severely underestimate ALAN in areas with a high level of LED lighting (Wang, Shrestha et al. 2022). Future studies need to use data from other imaging systems with broader spectral sensitivity, such as the images taken by the International Space Station and other satellites, to accurately characterize temporal trends in ALAN.

It is well established that ALAN is an indicator of economic and population growth (Levin, Kyba et al. 2020). As

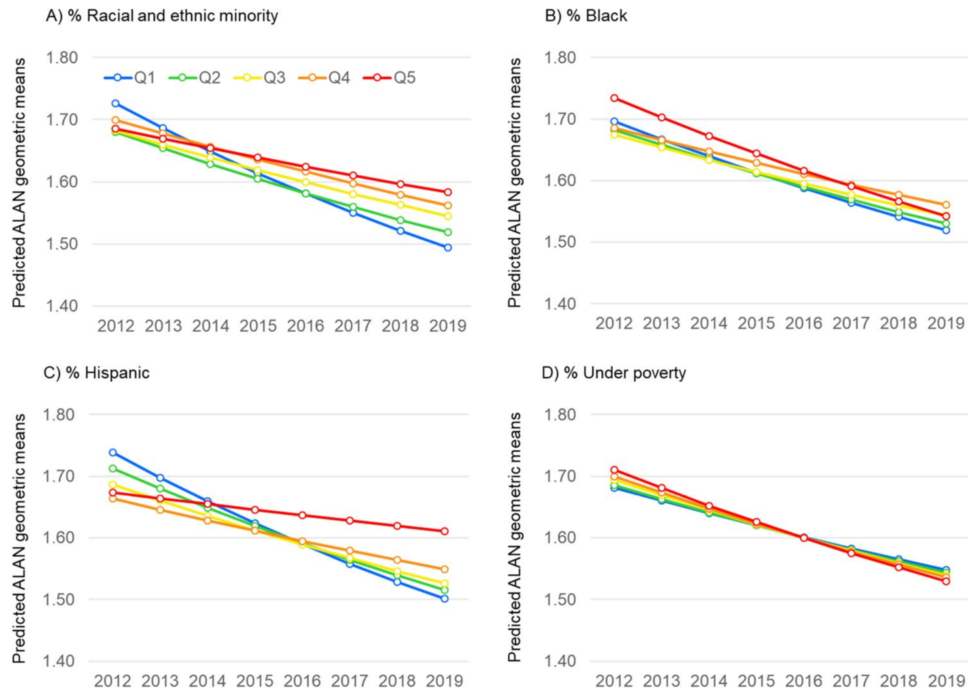

Fig. 3 ALAN trends (2012–2019, expressed in geometric means) in the contiguous US by **A** percent of racial/ethnic minority, **B** percent of Blacks, **C** percent of Hispanics, and **D** percent with a household income below the federal poverty line at county level. Q1–Q5 represent quintiles of each sociodemographic factors in each panel

expected, we found a positive correlation between changes in ALAN and changes in GDP and population size at the county level. However, we also found that trends in GDP and population only explained less than one-fourth of the total variability in temporal trends in ALAN in 2012–2019, suggesting other factors are in play. For example, we found that many rural counties in Texas experienced a dramatic increase in ALAN, and this pattern is most likely to be explained by increases in oil and gas drilling activities, particularly the bright light emitted from gas flares (Elvidge and Zhizhin 2021). The identification of specific driving forces underlying temporal changes is critical to developing ALAN surveillance programs and policy interventions.

Decades of EJ research focusing on characterizing the uneven distribution of environmental exposures in the population has long documented disproportionately high exposure levels to many environmental pollutants in disadvantaged populations. A recent EJ analysis using a one-time measurement of ALAN in 2014 reported that minority populations in the USA had a higher population-weighted mean exposure to light pollution when compared to non-Hispanic White Americans (Nadybal, Collins et al. 2020). We expanded this line of research by, for the first time, reporting different trajectories of ALAN across counties with different racial/ethnic compositions. Counties with the highest concentration of White populations experienced the most rapid decline in ALAN, while counties with a higher % of minority populations, particularly Hispanic populations, experienced significantly less decline between 2012 and 2019. The reduced decline in ALAN among Hispanic populations may be explained by the larger Hispanic populations residing in areas with stable or even an increase in ALAN, such as counties in California and Texas. This finding suggests that the disparities in ALAN are dynamic, and thus, characterizing temporal changes is key to a better understanding and predicting ALAN burdens across the population. The widening gaps in racial/ethnic disparities in ALAN are alarming and warrant further investigation. In particular, future studies should focus on identifying underlying contributing factors, including economic development, urban planning, and the transition to LED technology, and quantifying the potential economic, social, and public health implications of ALAN disparities.

Growing attention has been directed to the negative impacts of light pollution on energy consumption, greenhouse gas emissions, ecology, evolution, and human health. The US Energy Information Administration estimated that in 2021 lighting accounted for about 5% of total US electricity consumption (Duncan, Geigert et al. 2018), and efforts in curbing light pollution often point to reducing energy expenditure and cost as a main motivation to develop more efficient artificial lighting. However, the emphasis on energy expenditure of lighting technology alone ignores the myriad unintended consequences of lighting itself. Almost all species on Earth possess an endogenous circadian timing system, which plays a critical role in orchestrating numerous biological processes and represents a fundamental adaptation to the 24-h cycle of the natural lighting environment on our planet (Albrecht 2010). Light pollution alters the natural light-and-dark cycle, disrupts circadian rhythms, and has been shown to have adverse effects on the survival, reproduction, migration, communication, and general health and well-being of many taxa, including both nocturnal and diurnal organisms (Jägerbrand and Bouroussis 2021).

In humans, pervasive exposure to ALAN suppresses melatonin, a key hormone in circadian regulation, and enables nighttime activities that are misaligned with the internal circadian clock (Lunn, Blask et al. 2017). Both melatonin suppression and misaligned nighttime activities can lead to circadian disruption and sleep deficiencies, which are important risk factors for a wide range of adverse health outcomes (Roenneberg and Merrow 2016). Epidemiological studies have linked excessive ALAN with a wide range of health conditions (Lunn, Blask et al. 2017, Mason, Boubekri et al. 2018), including mental disorders (Paksarian, Rudolph et al. 2020), weight gain (Park, White et al. 2019), obesity risk (Zhang, Jones et al. 2020), postmenopausal breast cancer (Hurley, Goldberg et al. 2014, James, Bertrand et al. 2017, Xiao, James et al. 2020, Xiao, Gierach et al. 2021), and pancreatic, thyroid, and prostate cancers (Kim, Lee et al. 2017, Xiao, Jones et al. 2021, Zhang, Jones et al. 2021). Although the observational nature of these epidemiological investigations makes it challenging to establish causal relationships between ALAN and health outcomes, the role of ALAN in disease risk is further supported by numerous laboratory studies in both animal models and human subjects that convincingly show a mechanistic link between misaligned light exposure, circadian disruption, and adverse health effects (Opperhuizen, Stenvers et al. 2017, Fleury, Masis-Vargas et al. 2020, Mason, Grimaldi et al. 2022). Taken together, ALAN is an important environmental exposure with significant consequences in public health and other areas, and thus, it is imperative to generate comprehensive and up-to-date ALAN data to enable better assessment of the population burden of ALAN exposure.

It is worth noting that although there are significant implications of our current analysis, an important limitation of mapping ALAN using satellite imagery in the context of public health is the uncertainty about how well satellite-based ALAN estimates capture actual light exposure experienced at the individual level. Satellite-based measures are primarily driven by outdoor ALAN levels and may not accurately reflect indoor light exposure that may have a larger and more direct health impact for most individuals. Indeed, two previous studies reported minimal correlation between the satellite-based estimates and individual-level measures of LAN (Rea, Brons et al. 2011, Huss, van Wel et al. 2019). Moreover, the validity of using satellite-based LAN estimates as a proxy measure of individual-level LAN exposure can be influenced by individual lifestyle and occupational factors (e.g., window treatment, sleep habits, nighttime social activities, shift work) and can vary among groups with different sociodemographic and geographic characteristics. Therefore, the field will benefit from large-scale validation study aimed at comparing satellite-based estimates of LAN with individual-level measures and in-depth investigation into how population attributes may influence the validity of satellite-based LAN measure in the context of public health research.

Another limitation of the current study is that by analyzing average ALAN at the county level, the results do not reflect within county variation in the spatiotemporal distribution of ALAN and thus cannot be used to identify smaller geographic areas (e.g., census tract, block, small neighborhood) with high levels of and/or rapid increase in ALAN exposures. We chose county as the unit of analysis for the current study because it corresponds to the administrative level for public health monitoring and policy-making. However, it would be important for public health researchers and practitioners to recognize the potentially vast difference in ALAN exposure within a county to accurately identify vulnerable communities and employ policy interventions. In addition, another factor that may have an important influence on the population burden of ALAN is the mobility pattern, which determines the cumulative exposure to ALAN and its long-term health effects. Although studying the impact of mobility pattern on ALAN exposure is beyond the scope of this study, the field will benefit from future studies that track ALAN exposure levels over time in a population.

In summary, our analysis demonstrated substantial differences in both geographic distribution and temporal trends of ALAN in US counties. The results also highlighted evolving disparities in ALAN exposure across different racial/ethnic groups. Given the broad implications of ALAN, including its well-established public health consequences, future studies should closely monitor ALAN exposure, evaluate attributable health burdens, and provide evidence for developing targeted policies to ameliorate the negative societal impact of ALAN.

Supplementary Information The online version contains supplementary material available at https://doi.org/10.1007/s11356-023-30572-y.

Author contribution Conceptualization: QX and CB; data curation and analysis: QX, MZ, YL, JL, KZ, and CB; writing-original draft: QX; writing-reviewing and editing: QX, MZ, YL, JL, KZ, MF, JW, and CB. All authors read and approved the final manuscript.

Funding This study is supported by 80NSSC21K0510 from the National Aeronautics and Space Administration Health and Air Quality Applied Science Team.

Data Availability County-level ALAN data are now published and publicly available (https://disc.gsfc.nasa.gov/datasets/ALAN_VIIRS_CONUS_1/summary).

Declarations

Ethics approval Not applicable.

Consent to participate Not applicable.

Consent to publish Not applicable.

Competing interests The authors declare no competing interests.

References

Albrecht U (2010) The circadian clock. Springer Science & Business Media

Cao C, Bai Y (2014) Quantitative analysis of VIIRS DNB nightlight point source for light power estimation and stability monitoring. Remote Sens 6(12):11915–11935

Duncan, B. N., M. Geigert and L. Lamsal (2018). "A brief tutorial on using the ozone monitoring instrument (OMI) nitrogen dioxide (NO2) data product for SIPS preparation."

Elvidge, C. and M. J. O. D. Zhizhin (2021). "Global gas flare survey by infrared imaging, VIIRS Nightfire, 2012-2019."

Elvidge CD, Hsu F-C, Zhizhin M, Ghosh T, Taneja J, Bazilian MJRS (2020) Indicators of electric power instability from satellite observed nighttime lights. Remote Sens 12(19):3194

Falchi F, Cinzano P, Elvidge CD, Keith DM, Haim A (2011) Limiting the impact of light pollution on human health, environment and stellar visibility. J Environ Manag 92(10):2714–2722

Falchi F, Cinzano P, Duriscoe D, Kyba CC, Elvidge CD, Baugh K, Portnov BA, Rybnikova NA, Furgoni R (2016) The new world atlas of artificial night sky brightness. Sci Adv 2(6):e1600377

Falchi F, Furgoni R, Gallaway TA, Rybnikova NA, Portnov BA, Baugh K, Cinzano P, Elvidge CD (2019) Light pollution in USA and Europe: the good, the bad and the ugly. J Environ Manag 248:109227

Fleury G, Masis-Vargas A, Kalsbeek A (2020) Metabolic implications of exposure to light at night: lessons from animal and human studies. Obesity (Silver Spring) 28(Suppl 1):S18–S28

Gaston KJ, Visser ME, Holker F (2015) The biological impacts of artificial light at night: the research challenge. Philos Trans R Soc Lond Ser B Biol Sci 370(1667)

Hölker F, Moss T, Griefahn B, Kloas W, Voigt CC, Henckel D, Hänel A, Kappeler PM, Völker S, Schwope A (2010) The dark side of light: a transdisciplinary research agenda for light pollution policy. Ecol Soc 15(4)

Hurley S, Goldberg D, Nelson D, Hertz A, Horn-Ross PL, Bernstein L, Reynolds P (2014) Light at night and breast cancer risk among California teachers. Epidemiology 25(5):697–706

Huss A, van Wel L, Bogaards L, Vrijkotte T, Wolf L, Hoek G, Vermeulen R (2019) Shedding some light in the dark-a comparison of personal measurements with satellite-based estimates of exposure to light at night among children in the Netherlands. Environ Health Perspect 127(6):67001

Jägerbrand, A. K. and C. A. J. S. Bouroussis (2021). "Ecological impact of artificial light at night: effective strategies and measures to deal with protected species and habitats." 13(11): 5991.

James P, Bertrand KA, Hart JE, Schernhammer ES, Tamimi RM, Laden F (2017) Outdoor light at night and breast cancer incidence in the Nurses' Health Study II. Environ Health Perspect 125(8):087010

Kim KY, Lee E, Kim YJ, Kim J (2017) The association between artificial light at night and prostate cancer in Gwangju City and South Jeolla Province of South Korea. Chronobiol Int 34(2):203–211

Kyba CCM, Kuester T, Sanchez de Miguel A, Baugh K, Jechow A, Holker F, Bennie J, Elvidge CD, Gaston KJ, Guanter L (2017) Artificially lit surface of Earth at night increasing in radiance and extent. Sci Adv 3(11):e1701528

Levin N, Kyba CCM, Zhang Q, Sánchez de Miguel A, Román MO, Li X, Portnov BA, Molthan AL, Jechow A, Miller SD, Wang Z, Shrestha RM, Elvidge CD (2020) Remote sensing of night lights: a review and an outlook for the future. Remote Sens Environ 237:111443

Li X, Elvidge C, Zhou Y, Cao C, Warner T (2017) Remote sensing of night-time light. Int J Remote Sens 38(21):5855–5859

Lunn RM, Blask DE, Coogan AN, Figueiro MG, Gorman MR, Hall JE, Hansen J, Nelson RJ, Panda S, Smolensky MH, Stevens RG, Turek FW, Vermeulen R, Carreon T, Caruso CC, Lawson CC, Thayer KA, Twery MJ, Ewens AD et al (2017) Health consequences of electric lighting practices in the modern world: a report on the National Toxicology Program's workshop on shift work at night, artificial light at night, and circadian disruption. Sci Total Environ 607-608:1073–1084

Mason IC, Boubekri M, Figueiro MG, Hasler BP, Hattar S, Hill SM, Nelson RJ, Sharkey KM, Wright KP, Boyd WA, Brown MK, Laposky AD, Twery MJ, Zee PC (2018) Circadian health and light: a report on the National Heart, Lung, and Blood Institute's Workshop. J Biol Rhythm 33(5):451–457

Mason IC, Grimaldi D, Reid KJ, Warlick CD, Malkani RG, Abbott SM, Zee PC (2022) Light exposure during sleep impairs cardiometabolic function. Proc Natl Acad Sci U S A 119(12):e2113290119

Moschandreas, D. (2011). "Models of human exposure to environmental contaminants."

Nadybal SM, Collins TW, Grineski SE (2020) Light pollution inequities in the continental United States: a distributive environmental justice analysis. Environ Res 189:109959

Opperhuizen AL, Stenvers DJ, Jansen RD, Foppen E, Fliers E, Kalsbeek A (2017) Light at night acutely impairs glucose tolerance in a time-, intensity- and wavelength-dependent manner in rats. Diabetologia 60(7):1333–1343

Ou J, Liu X, Li X, Li M, Li W (2015) Evaluation of NPP-VIIRS nighttime light data for mapping global fossil fuel combustion CO2 emissions: a comparison with DMSP-OLS nighttime light data. PLoS One 10(9):e0138310

Paksarian D, Rudolph KE, Stapp EK, Dunster GP, He J, Mennitt D, Hattar S, Casey JA, James P, Merikangas KR (2020) Association of outdoor artificial light at night with mental disorders and sleep patterns among US adolescents. JAMA Psychiatry 77(12):1266–1275

Park YM, White AJ, Jackson CL, Weinberg CR, Sandler DP (2019) Association of exposure to artificial light at night while sleeping with risk of obesity in women. JAMA Intern Med 179(8):1061–1071

Rea MS, Brons JA, Figueiro MG (2011) Measurements of light at night (LAN) for a sample of female school teachers. Chronobiol Int 28(8):673–680

Roenneberg T, Merrow M (2016) The circadian clock and human health. Curr Biol 26(10):R432–R443

Román MO, Wang Z, Sun Q, Kalb V, Miller SD, Molthan A, Schultz L, Bell J, Stokes EC, Pandey B, Seto KC, Hall D, Oda T, Wolfe RE, Lin G, Golpayegani N, Devadiga S, Davidson C, Sarkar S et al (2018) NASA's Black Marble nighttime lights product suite. Remote Sens Environ 210:113–143

Song J, Wang J, Xia X, Lin R, Wang Y, Zhou M, Fu D (2021) Characterization of urban heat islands using city lights: insights from MODIS and VIIRS DNB observations. Remote Sens 13(16):3180

Tan X, Zhu X, Chen J, Chen R (2022) Modeling the direction and magnitude of angular effects in nighttime light remote sensing. Remote Sens Environ 269:112834

Voelkel J, Hellman D, Sakuma R, Shandas V (2018) Assessing vulnerability to urban heat: a study of disproportionate heat exposure and access to refuge by socio-demographic status in Portland, Oregon. Int J Environ Res Public Health 15(4)

Wang Z, Shrestha RM, Román MO, Kalb VLJIG, Letters RS (2022) NASA's black marble multiangle nighttime lights temporal composites. IEEE Geosci Remote Sens Lett 19:1–5
Xiao Q, James P, Breheny P, Jia P, Park Y, Zhang D, Fisher JA, Ward MH, Jones RR (2020) Outdoor light at night and postmenopausal breast cancer risk in the NIH-AARP diet and health study. Int J Cancer 147(9):2363–2372
Xiao Q, Gierach GL, Bauer C, Blot WJ, James P, Jones RR (2021a) The association between outdoor artificial light at night and breast cancer risk in Black and White women in the Southern Community Cohort Study. Environ Health Perspect 129(8):87701
Xiao Q, Jones RR, James P, Stolzenberg-Solomon RZ (2021b) Light at night and risk of pancreatic cancer in the NIH-AARP Diet and Health Study. Cancer Res 81(6):1616–1622
Zhang D, Jones RR, Powell-Wiley TM, Jia P, James P, Xiao Q (2020) A large prospective investigation of outdoor light at night and obesity in the NIH-AARP Diet and Health Study. Environ Health 19(1):74
Zhang D, Jones RR, James P, Kitahara CM, Xiao Q (2021) Associations between artificial light at night and risk for thyroid cancer: a large US cohort study. Cancer 127(9):1448–1458